CrossMark

BREAST

Early prediction of response to neoadjuvant chemotherapy in breast cancer patients: comparison of single-voxel [1]H-magnetic resonance spectroscopy and ^{18}F-fluorodeoxyglucose positron emission tomography

Nariya Cho[1,2,3] · Seock-Ah Im[4] · Keon Wook Kang[5,6] · In-Ae Park[7] ·
In Chan Song[1] · Kyung-Hun Lee[4] · Tae-Yong Kim[4] · Hyunjong Lee[5] ·
In Kook Chun[5,8] · Hai-Jeon Yoon[5,9] · Woo Kyung Moon[1,2,3]

Abstract

Objectives To prospectively compare performances of single-voxel proton magnetic resonance spectroscopy (^{1}H-MRS) and ^{18}F-fluorodeoxyglucose positron emission tomography (FDG-PET) in predicting pathologic response to neoadjuvant chemotherapy (NAC) in breast cancer patients.

Methods Thirty-five breast cancer patients who received NAC and subsequent surgery were prospectively enrolled. MRS and FDG-PET were performed before and after the 1st NAC cycle. Percentage changes of total choline-containing compounds (tCho) via MRS, and maximum and peak standardized uptake values (SUV_{max}, SUV_{peak}) and total lesion glycolysis (TLG) via FDG-PET were measured, and their performances in predicting pathologic complete response (pCR) were compared.

Results Of the 35 patients, 6 showed pCR and 29 showed non-pCR. Mean % reductions of tCho, SUV_{max}, SUV_{peak}, and TLG of the pCR group were larger than those of the non-pCR group (-80.3±13.9 % vs. -32.1±49.4 %, $P=0.025$; -54.7±22.1 % vs. -26.3±33.7 %, $P=0.058$; -60.7±18.3 % vs. -32.3±23.3 %, $P=0.009$; -89.5± 8.5 % vs. -52.6±36.2 %, $P=0.020$). Diagnostic *accuracy* (area under ROC curve; Az, 0.911) of the % reduction of tCho was comparable to those of %SUV_{max} (0.822), SUV_{peak} (0.862), and TLG (0.879) in distinguishing pCR from non-pCR (all $P>0.05$).

Conclusion MRS showed comparable performance to FDG-PET in early prediction of pCR in breast cancer patients.

Key points
• *MRS can predict response to NAC in breast cancer post-1st cycle.*
• *Changes in tCho and SUV after NAC reflect tumour cellularity changes.*
• *MRS can be an alternative to FDG-PET in predicting response to NAC.*

✉ Woo Kyung Moon
moonwk@snu.ac.kr

[1] Department of Radiology, Seoul National University Hospital, 101 Daehak-ro, Jongno-gu Seoul 110-744, Republic of Korea

[2] Department of Radiology, Seoul National University College of Medicine, 103 Daehak-ro, Jongno-gu Seoul 110-799, Republic of Korea

[3] Institute of Radiation Medicine, Seoul National University Medical Research Center, Seoul, Republic of Korea

[4] Department of Internal Medicine, Seoul National University Hospital, Seoul, Republic of Korea

[5] Department of Nuclear Medicine, Seoul National College of Medicine, Seoul, Republic of Korea

[6] Cancer Research Institute, Seoul National University, Seoul, Republic of Korea

[7] Department of Pathology, Seoul National University Hospital, Seoul, Republic of Korea

[8] Department of Nuclear Medicine, School of Medicine, Kangwon National University, Chuncheon, Gangwon-do, Republic of Korea

[9] Department of Nuclear Medicine, Ewha Woman's University, Seoul, Republic of Korea

Springer

Abbreviations

NAC	Neoadjuvant chemotherapy
H-MRS	Proton magnetic resonance spectroscopy
FDG-PET	[18]F- fluorodeoxyglucose positron emission tomography
pCR	Pathologic complete response
MRI	Magnetic resonance imaging
tCho	Total choline-containing compounds
SUV	Standardized uptake value
TLG	Total lesion glycolysis

Introduction

Neoadjuvant chemotherapy (NAC) prior to surgery is
not only the recommended standard treatment for locally
advanced breast cancer [1], but is also used in patients
with operable breast cancers in order to increase breast-
conservation rates [2]. In this regard, it has previously
been shown that achieving pathologic complete response
(pCR) after NAC is significantly associated with
favourable disease-free survival outcomes [3]. However,
as 20 % of patients are resistant to NAC, prediction of
its response at the initial cycles, which would allow the
treatment to be modified in non-responders, would be of
great clinical significance [4]. Indeed, a recent study has
reported that the survival rates of non-responders to ini-
tial NAC who responded to a different regimen, were
similar to those of responders to the initial regimen [5].

For the prediction of pCR during the early cycles of
NAC, tumour size or volume change measured on
contrast-enhanced magnetic resonance imaging (MRI)
has been demonstrated to be superior to clinical assess-
ment [6]. However, as changes of tumour size after
treatment usually occur after the 2nd cycle of NAC
[7], earlier predictors reflecting angiogenesis, metabolic
activity, or tumour cellularity, which may show change
before tumour shrinkage, have been explored. [18]F-
fluorodeoxyglucose (FDG)-positron emission tomogra-
phy (PET) has been reported to show 65–88-% accuracy
in the prediction of pathologic response after the first or
second cycle of NAC [8, 9]. In addition, greater total
choline-containing compounds (tCho) signal changes of
the tumour via in vivo proton magnetic resonance spec-
troscopy (^{1}H-MRS) have been observed in patients with
pCR than in non-pCR patients also after only the first
or second cycle of NAC [10–12]. Furthermore, Tozaki

et al. reported that the changes in the integral value of
the tCho peak determined via MRS were correlated with
those of peak standardized uptake values (SUVs) deter-
mined via FDG-PET, both during and following NAC
cycles [13].

However, to the best of our knowledge, there have
been no studies comparing the performances of MRS
and FDG-PET in predicting the pathological responses to
NAC. Thus, the purpose of our study was to prospectively
compare the performances of single-voxel ^{1}H-MRS and
FDG-PET in predicting the pathologic response to NAC
in breast cancer patients.

Methods

Patients

The institutional review board of our hospital approved
this prospective study and written informed consent was
obtained from all patients. Between August 2010 and De-
cember 2012, 57 stage II or stage III breast cancer patients
who received NAC were enrolled according to criteria
described in a previous study [14]: patients with (a) breast
cancer pathologically confirmed by core needle biopsy, (b)
an initial clinical stage of II or III, (c) objectively measur-
able lesions, (d) Eastern Cooperative Oncology Group per-
formance scores of 0-2, (e) previously untreated and (f)
adequate bone marrow, and hepatic, cardiac and renal
function. The patients received 6 cycles of neoadjuvant
docetaxel (75 mg/m^2; Taxotere; Sanofi Aventis, Paris,
France) with doxorubicin (50 mg/m^2; Adriamycin PFS;
Ildong Pharmaceutical Co., Seoul, Korea) or 4 cycles of
doxorubicin (60 mg/m^2) with cyclophosphamide (600 mg/m^2; ;
Endoxane; Baxter, Deerfield, IL) followed by 4 cycles of
docetaxel (75 mg/m^2), which is the standard NAC protocol
at our institution. All patients were clinically examined prior
to each cycle of chemotherapy and the regimen was con-
tinued if there was no evidence of progression. Their re-
sponse was evaluated at the completion of chemotherapy
and curative surgery was performed. Each patient
underwent both MRS and FDG-PET twice: one examina-
tion each within 3 weeks prior to chemotherapy and a
second examination 2 weeks after the first cycle of chemo-
therapy but prior to the second cycle of chemotherapy. The
reason for the second examination performed at post-1st
cycle of chemotherapy was that predicting response at an
earlier time point was highly important to modify the treat-
ment for non-responders.

Of the 57 patients enrolled, 22 patients were excluded as no
MRS data were obtained ($n=13$), or due to withdrawal of
consent ($n=3$), an inconsistent MR protocol ($n=4$) or with-
drawal from surgery ($n=2$). Thus, 35 patients (mean age,

46.9 years; range, 35–65 years) with invasive breast cancers (mean size, 4.8 cm; range 2.3–11.5 cm measured at baseline contrast-enhanced MRI) were finally included for analysis. The patients had invasive ductal carcinomas (94.3 %) or invasive lobular carcinoma (5.7 %) with a clinical stage of II (22.9 %) or III (77.1 %).

^{1}H-MR spectroscopy and image analysis

Single-voxel ^{1}H-MRS examinations were performed with patients in the prone position using a 3.0-Tesla scanner (Verio; Siemens Medical Solutions, Erlangen, Germany) with a dedicated 16-channel breast coil equipped with a bottle phantom (syngo GRACE external phantom; Siemens Medical Solutions, Erlangen, Germany) for external reference [15]. The phantom filled with 1.25 g of $NiSO_46H_2O$ per 1,000 g of H_2O was placed behind the breast coil. After obtaining contrast-enhanced MR examinations, sagittal, coronal, and axial T1-weighted localizer images were acquired and used for voxel placement. After a $20\times20\times20$-mm^3 voxel was placed in the tumour, a point-resolved spectroscopy sequence (PRESS) with a repetition time/echo time (TR/TE) of 6,000/125 msec, a spectral width of 2,000 Hz, and 2,048 data points were performed. The acquisition time was 8 minutes and 12 seconds. Following the first chemotherapy, when a tumour decreased less than 2 cm, a $10\times10\times10$-mm^3 voxel was used. Semiautomatic shimming was performed to achieve full width at half maximum of the unsuppressed water peak of 10 to 25 Hz. For the acquisition of water- and fat-suppressed data, 160 scans with a TR of 3,000 msec were obtained. For semi-quantification of the choline signal, water-unsuppressed data were obtained using 4 scans with a TR of 6,000 msec from a $10\times10\times10$-mm^3 voxel in an external water bottle.

Each spectrum was analyzed using syngo software (Siemens Medical Solutions, Erlangen, Germany) at an MR workstation. Hanning filtering with a width of 400 msec and zero filling of 4,096 was applied before the Fourier transform (FT). Final spectra were obtained using phase and polynomial baseline corrections. Areas of choline signals were estimated by applying Gaussian model fitting and their values were normalized via the normalization procedure using the external water reference signal as performed in a previous study [15]. The presence of a tCho signal was defined as a peak at 3.2 ppm clearly identifiable from the baseline noise. The integral values of the tCho signals were calculated and recorded.

^{18}F-FDG PET image acquisition

FDG-PET images were obtained using an integrated PET/computed tomography (CT) system (Biograph 40, Siemens Medical Solutions, Erlangen, Germany). After the patients fasted for at least 6 hours, ^{18}F-FDG (5.18 kBq/g) was intravenously injected and PET/CT scanning was initiated 1 hour later. CT scans were performed for attenuation correction and anatomical reference from the base of skull to the proximal thigh followed by an emission scan for a period of 2 minutes per bed. An iterative algorithm was used to reconstruct the PET image. The SUV, defined as the tissue concentration of radioactivity (kBq/mL) divided by the injected dose per body weight (kBq/g), was measured by three nuclear medicine physicians (H.L., H.J.Y., I.K.C.) in consensus using a dedicated software (syngo.via, Siemens Medical Solutions, Erlangen, Germany). After a volume of interest (VOI) was drawn over the breast lesion, the maximal SUV (SUV_{max}), defined as the value of the highest pixel, and the peak SUV (SUV_{peak}), defined as the highest mean value of SUV in a 1 cm^3 spherical VOI, were measured. After an isoactivity contour was drawn in the VOI using a preset margin threshold, and the metabolic tumor volume (MTV, cm^3), mean SUV (SUV_{mean}) of the MTV, and total lesion glycolysis (TLG) defined as MTV multiplied by SUV_{mean} were calculated [16–18]. For the margin threshold, SUV_{max} 2.0 was used, which was performed in a previous study for breast cancer [18].

Histopathologic analysis

Core biopsy specimens obtained prior to chemotherapy as well as surgical specimens were evaluated by an experienced pathologist (I.A.P.) with 29 years of experience in breast histopathology to determine pathological response and to quantify changes in tumour cellularity. The Miller-Payne system was used to classify the changes in tumour cellularity after chemotherapy [19]: grade 1 = no reduction of cellularity, grade 2 = loss of tumour cells up to 30 %, grade 3 = 30–90 % reduction, grade 4 = more than 90 % reduction, and grade 5 = pCR, defined as the absence of invasive tumour cells, although ductal carcinoma in situ may have been present. Miller-Payne grades of 3, 4 or 5 were defined as showing good pathologic response and grades 1 or 2 were defined as showing minor response [20].

Tumour diameters and expressions of the oestrogen receptor (ER), progesterone receptor (PR) and human epidermal growth factor receptor (HER)-2 were evaluated based on the surgical histopathology. Standardized templates were used to record the number and sizes of the invasive components and carcinoma in in situ components of the tumour and the status of lymph node metastasis. For lesions showing pCR, the expressions of ER, PR, and HER-2 were determined based on the core biopsy specimens. A cut-off value of 10 % was used to define positivity for ER and PR at 10X magnification. HER-2 expression was categorized as 0, 1+, 2+ or 3+ through immunohistochemical staining. Tumours with a score of 3+ were categorized as HER-2 positive, and tumours with a score of 0 or 1+ as HER-2 negative. For tumours with a score of 2+, fluorescence in situ hybridization was performed. When the

ratio of HER-2 gene copies to chromosome 17 signals was >2.2, HER-2 expression was considered positive. Tumours were classified as hormone receptor-positive (e.g., ER-positive or PR-positive), triple negative (e.g., hormone receptor-negative and HER-2-negative) or HER-2-positive (e.g., HER-2-positive and hormone receptor-negative) based on the immunohistochemical staining.

Statistical analysis

Fisher's exact test was performed to compare the clinicopathologic variables (age at diagnosis, clinical stage, expression of ER, PR, HER-2 and the Ki-67 protein, immunohistochemical subtype, chemotherapy regimen, and type of surgery) of the pCR and non-pCR groups as well as the good-response and minor-response groups. An independent samples t-test was performed to compare imaging variables (mean tumour size, mean tumour volume, integral value of the tCho signal, SUV_{max}, SUV_{peak}, and TLG) between the pCR and non-pCR groups as well as the good-response and minor-response groups. Linear regression analysis was performed to evaluate the correlation between imaging parameters and Miller-Payne grades of cellular reduction.

Area under the receiver operating characteristic (ROC) curve analysis was performed to compare the diagnostic performance of MRS and FDG-PET in the prediction of non-pCR. To suggest the optimal criteria for prediction, the best cut-off values of the MRS and FDG-PET to achieve the maximal sum of sensitivity (proportion of pathologic non-responders correctly classified as non-responders) and specificity (proportion of pathologic responders correctly classified as responders) were determined. Thereafter, sensitivity, specificity, positive predictive value (PPV) and negative predictive value (NPV) for the prediction of non-pCR or minor responses were calculated.

All statistical analyses were performed using the Statistical Program for Social Sciences software (version 19.0; SPSS, Chicago, IL) and MedCalc (version 10.3.0; MedCalc Software, Mariakerke, Belgium). A two-tailed P value of less than 0.05 was considered to indicate a statistically significant difference.

Results

The initial clinical stages of the patients were stage II in 8 of 35 patients (22.9 %) and stage III in 27 of 35 patients (77.1 %). The median interval between the MRS and FDG-PET examinations was 0 days (range, 0 to 4 days). Nineteen (55.9 %) of the 35 patients underwent MRS and FDG-PET examinations on the same day. The median interval between baseline imaging examination and the beginning of NAC was 4 days (range, 1–15 days). The median interval between baseline and the second imaging examination was 20 days for MRS and 21 days for FDG-PET examinations (both ranges, 14–36 days).

After surgery, pCR was achieved in 6 of the 35 patients (17.1 %). According to the Miller-Payne system, 28 patients were classified as good responders (80.0 %, grades 3 4, or 5), and 7 patients as minor responders (20.0 %, grades 1 or 2; Table 1). No differences were found in mean baseline tumour size between patients who showed pCR [4.5±1.7 cm (standard deviation, SD)] and patients with non-pCR (4.8±1.9 cm; P=0.736; Table 2). Following the first cycle of chemotherapy, a mean of 17.7±19.2 % in tumour diameter was decreased and a mean of 24.5±32.8 % in tumour volume was decreased. The pCR group showed a more decreased tumour diameter than the non-pCR group (-38.5±13.4 vs. -13.4±16.8 %, P=0.002) and the good-response group showed a more decreased tumour diameter than the minor-response group (-20.2±20.0 vs. -7.9±6.8 %, P=0.012; Table 2). The mean integral value of tCho of the 35 patients decreased from 13.7 (range, 2.3 to 56.4) to 7.0 (range, 0 to 21.9; P<0.001) and the mean SUV_{max} decreased from 12.2 (range, 3.8 to 35.3) to 8.0 (range, 2.2 to 30.4; P<0.001). The mean % reduction of tCho of the pCR group was significantly greater than that of the non-pCR group (-80.3±13.9 % vs. -32.1±49.4 %, P=0.025; Table 2; Figs. 1 and 2). The mean % reductions of SUV_{max}, SUV_{peak}, and TLG of the pCR group were also greater than those of the non-pCR group (SUV_{max}: -54.7± 22.1 % vs. -26.3±33.7 %, P=0.058; SUV_{peak}: -60.7± 18.3 % vs. -32.3±23.3 %, P=0.009; TLG: -89.5±8.5 % vs. -52.6±36.2 %, P=0.020; Table 2; Figs. 1 and 2).

With regard to the linear regression analysis between imaging parameters and grades of cellular reduction of tumours, % change of tumour size (r=-0.54, P=0.001), % change of tCho (r=-0.60, P<0.001), % change of SUV_{max} (r=-0.45, P=0.006), % change of SUV_{peak} (r=-0.60, P<0.001), and % change of TLG (r=-0.53, P=0.001) and the Miller-Payne grade showed correlations with statistical significance, which indicates that a greater reduction of tumour size, tCho, SUV_{max}, SUV_{peak}, or TLG results in less tumour cellularity remaining (Fig. 3).

In the prediction of pathological residual tumours, the area under the ROC curve of % change of tCho [0.911, 95 % confidence interval (CI), 0.765 to 0.980] was similar to those of % change of SUV_{max} (0.822, 95 % CI, 0.656 to 0.930, P=0.552), SUV_{peak} (0.862, 95 % CI, 0.703 to 0.955, P=0.675), and TLG (0.879, 95 % CI, 0.725 to 0.965, P=0.551; Fig. 4). If the best cut-off value was defined as the value yielding a maximum sum of sensitivity and specificity from the ROC curve analysis, a 60.7-% reduction of tCho yielded a 75.9-% sensitivity (22/ 29 non-pCRs) and 100-% specificity (6/6 pCRs); a 62.3-% reduction of SUV_{max} yielded a 100-% sensitivity (29/29 non-pCRs) and a 66.7-% specificity (4/6 pCRs; Table 3, Fig. 5).

Table 1 Association between clinicopathologic characteristics and pathological response

Variables	pCR (n=6)	Non-pCR (n=29)	P	Good response (n=28)	Minor response (n=7)	P
Age at diagnosis (years)			0.602			0.166
≤40	2 (25.0)	6 (75.0)		8 (100)	0 (0)	
>40	4 (14.8)	23 (85.2)		20 (74.1)	7 (25.9)	
Clinical stage			0.602			1.0
II	2 (25.0)	6 (75.0)		7 (87.5)	1 (12.5)	
III	4 (14.8)	23 (85.2)		21 (7.8)	6 (22.2)	
Estrogen receptor			0.177			0.402
Negative	5 (27.8)	13 (72.2)		13 (72.2)	5 (27.8)	
Positive	1 (5.9)	16 (94.1)		15 (88.2)	2 (11.8)	
Progesterone receptor			1.0			1.0
Negative	5 (18.5)	22 (81.5)		21 (77.8)	6 (22.2)	
Positive	1 (12.5)	7 (87.5)		7 (87.5)	1 (12.5)	
HER-2§			1.0			0.340
Negative	5 (19.2)	21 (80.8)		22 (84.6)	4 (15.4)	
Positive	1 (11.1)	8 (88.9)		6 (66.7)	3 (33.3)	
Ki-67			0.367			1.0
≤14 %	2 (10.0)	18 (90.0)		16 (80.0)	4 (20.0)	
>14 %	4 (26.7)	11 (73.3)		12 (80.0)	3 (20.0)	
Immunohistochemical subtype			0.102			0.117
Hormone receptor-positive	2 (11.1)	16 (88.9)		16 (88.9)	2 (11.1)	
Triple negative	4 (28.6)	7 (71.4)		9 (81.8)	2 (18.2)	
HER-2-positive	0 (0)	6 (100)		3 (50.0)	3 (50.0)	
Chemotherapy regimen			0.827			
Docetaxel/doxorubicin	3 (15.0)	17 (85.0)		16 (80.0)	4 (20.0)	0.392
Doxorubicin/cyclophosphamide plus docetaxel	1 (20.0)	4 (80.0)		3 (60.0)	2 (40.0)	
AC	2 (20.0)	8 (80.0)		9 (90.0)	1 (10.0)	
Type of surgery			1.0			1.0
Breast-conserving	4 (17.4)	19 (82.6)		18 (78.3)	5 (21.7)	
Total mastectomy	2 (16.7)	10 (83.3)		10 (83.3)	2 (16.7)	

pCR Pathologic complete response. *HER-2* Human epidermal growth factor receptor 2.

Discussion

According to our study results, in the prediction of pathological residual tumours, the area under the ROC curve of the % change of tCho at MRS was 0.911 (95 % CI, 0.765 to 0.980), which was similar to those of the % change of SUV_{max} (0.822, 95 % CI, 0.656 to 0.930; $P=0.552$), SUV_{peak} (0.862, 95 % CI, 0.703 to 0.955, $P=0.675$), and TLG (0.879, 95 % CI, 0.725 to 0.965, $P=0.551$) as determined via FDG-PET. Moreover, the % change of tumour size ($r=-0.54$, $P=0.001$), the % change of tCho ($r=-0.60$, $P<0.001$), the % change of SUV_{max} ($r=-0.45$, $P=0.006$), % change of SUV_{peak} ($r=-0.60$, $P<0.001$), and % change of TLG ($r=-0.53$, $P=0.001$) were all significantly correlated with changes in tumour cellularity grades after NAC.

Of the imaging biomarkers for the early prediction of response to NAC in breast cancer patients, previous studies have shown that FDG-PET is the leading imaging modality with reports that the changes of SUV on FDG-PET during the early cycles of NAC is associated with the pathologic response rate [8, 9] and disease-free survival outcomes [21, 22]. With regard to MR imaging, changes of the transfer constant derived from pharmacokinetic modelling on dynamic contrast enhanced (DCE)-MRI has also been shown to be associated with pathologic response [23] or favourable survival outcomes [24]. In comparison, however, superior accuracy of FDG-PET compared to that of DCE-MRI [25] or the usefulness of the complementary use of FDG-PET and DCE-MRI has been reported [26–28]. Yet, although these previous studies have reported that the combined use of FDG-PET and DCE-MRI after the 1st cycle of NAC improved the prediction of pCR or disease-free survival in breast cancer patients, additional ionizing radiation and cost limited this combination in real clinical practice.

**Table 2** Association between imaging variables and pathological response

Variables	pCR ($n=6$)	Non-pCR ($n=29$)	P	Good response ($n=28$)	Minor response ($n=7$)	P
Mean tumor size						
Baseline (cm)	4.5±1.7 (2.6, 7.4)	4.8±1.9 (2.3, 11.5)	0.736	4.9±2.0 (2.3, 11.5)	4.3±1.3 (3.1, 6.7)	0.452
After the first NAC (cm)	2.9±1.4 (1.2, 4.9)	4.1±1.6 (1.2, 7.2)	0.076	3.9±1.7 (1.2, 7.2)	3.9±1.2 (2.6, 5.8)	0.975
% change in tumor size (%)	-38.5±13.4	-13.4±16.8	0.002	-20.2±20.0	-7.9±6.8	0.012
Mean tumor volume						
Baseline (cm^3)	16.7±17.0 (1.3, 46.2)	42.9±102.6 (0.8, 552.3)	0.541	42.5±104.6 (0.8, 552.3)	22.3±19.2 (5.6, 61.7)	0.618
After the first NAC (cm^3)	10.1±13.5 (1.0, 36.7)	27.3±47.6 (0.7, 232.6)	0.391	25.5±48.5 (0.7, 232.6)	19.7±18.6 (4.5, 58.5)	0.760
% change in tumor volume (%)	-34.4±42.9	-22.5±30.8	0.425	-27.1±35.6	-14.3±15.3	0.363
Integral value of tCho at MRS						
Baseline Choline$_+$	15.0±8.4 (3.9, 28.1)	13.5±11.5 (2.3, 56.4)	0.755	14.2±11.6 (2.3, 56.4)	12.1±8.2 (2.4, 21.8)	0.657
Post-1st Choline	3.4±2.8 (0, 7.1)	7.8±6.3 (0, 21.9)	0.103	5.9±5.4 (0, 21.9)	11.6±6.6 (3.3, 21.2)	0.024
% change in choline (%)	-80.3±13.9	-32.1±49.4	0.025	-55.0±27.4	-18.0±71.6	0.036
SUV$_{max}$ at FDG-PET/CT						
Baseline	18.9±12.1 (4.1, 35.3)	10.7±5.6 (3.8, 26.1)	0.162	12.2±8.2 (3.8, 35.3)	11.8±4.0 (4.7, 15.1)	0.896
After the first NAC	9.7±10.7 (2.2, 30.4),	7.6±4.4 (2.4, 18.3),	0.647	7.4±6.1 (2.2, 30.4)	10.3±4.1 (4.4, 17.3)	0.246
% change in mean SUV$_{max}$ (%)	-54.7±22.1	-26.3±33.7	0.058	-37.0±30.3	-7.8±38.0	0.037
SUV$_{peak}$ at FDG-PET/CT						
Baseline	13.6±8.5 (3.0, 27.1)	7.7±4.5 (2.7, 19.5)	0.017	8.6±6.2 (2.7, 27.1)	8.9±3.0 (4.1, 13.5)	0.927
After the first NAC	5.8±6.4 (1.6, 18.6)	5.1±3.1 (1.5, 14.6)	0.673	4.7±3.9 (1.5, 18.6)	7.0±2.4 (3.0, 11.0)	0.150
% change in mean SUV$_{peak}$	-60.7±18.3	-32.3±23.3	0.009	-42.7±18.7	-15.3±34.9	0.007
TLG at FDG-PET/CT						
Baseline	184.2±200.1 (25.7, 466.7)	182.6±340.0 (4.5, 1535.4)	0.992	191.9±352.7 (4.5, 1535.4)	147.1±105.6 (41.3, 299.6)	0.744
After the first NAC	27.7±40.0 (0.3, 103.2)	66.9±95.2 (0, 391.2)	0.334	47.2±82.7 (0, 391.2)	112.0±100.8 (9.9, 270.6)	0.085
% change in mean TLG	-89.5±8.5 (-99.3, -77.9)	-52.6±36.2 (-100.0, 76.4)	0.020	-68.1±24.6 (-100.0, -2.2)	-22.5±51.4 (-79.9, 76.4)	0.058

Numbers represent the mean values and standard deviations with ranges in parentheses.

pCR Pathologic complete response. *NAC* Neoadjuvant chemotherapy. *HER-2* Human epidermal growth factor receptor 2. *SUV* standardized uptake value, *TLG* total lesion glycolysis.

In this regard, previous studies showing that MRS may have the potential to predict the pathologic response in the initial stages of chemotherapy has clear clinical implications as it may overcome the aforementioned limitations of PET while still providing the opportunity to minimize ineffective or toxic treatment or provide more cycles of effective regiments with confidence. Indeed, changes in the tCho concentration of the tumour 24 hours after the 1st chemotherapy [10] session or at a time point between the 1st and 2nd chemotherapy had already been demonstrated [11, 12], similar to our study results. Moreover, given our linear regression analysis results and the demonstrated correlation between % tCho changes ($r=-0.60$, $P<0.001$) and % changes in SUV$_{max}$ ($r=-0.45$, $P=0.006$) observed after the 1st cycle of

Fig. 1 Single-voxel ^{1}H-MR spectroscopy and ^{18}F-FDG-PET of a 55-year-old woman with invasive ductal carcinoma (ER-, PR- and HER-2-positive) which demonstrated pCR after neoadjuvant chemotherapy and surgery. Pre-treatment (*A*) and post-1st cycle (*B*) single-voxel ^{1}H-MR spectrum shows that the normalized integral value of total choline-containing compound (tCho) resonance peak at 3.21 ppm decreased from 8.83 to 1.81, measured as a 79.6-% reduction. Pre-treatment (*C*) and post-1st cycle (*D*) SUV$_{max}$ of the tumour on FDG-PET decreased from 9.1 to 2.4, measured as a 73.6-% reduction. SUV$_{peak}$ of the tumour decreased from 7.2 to 1.7, measured as a 76.4-% reduction. Pre-treatment contrast-enhanced MRI (*E*) shows that the mass is 4.1 cm in diameter and preoperative contrast-enhanced MRI taken after completion of NAC shows the disappearance of the mass (*F*). Surgical histopathology revealed no residual tumour. Milller-Payne classification was a grade of 5, or complete response.
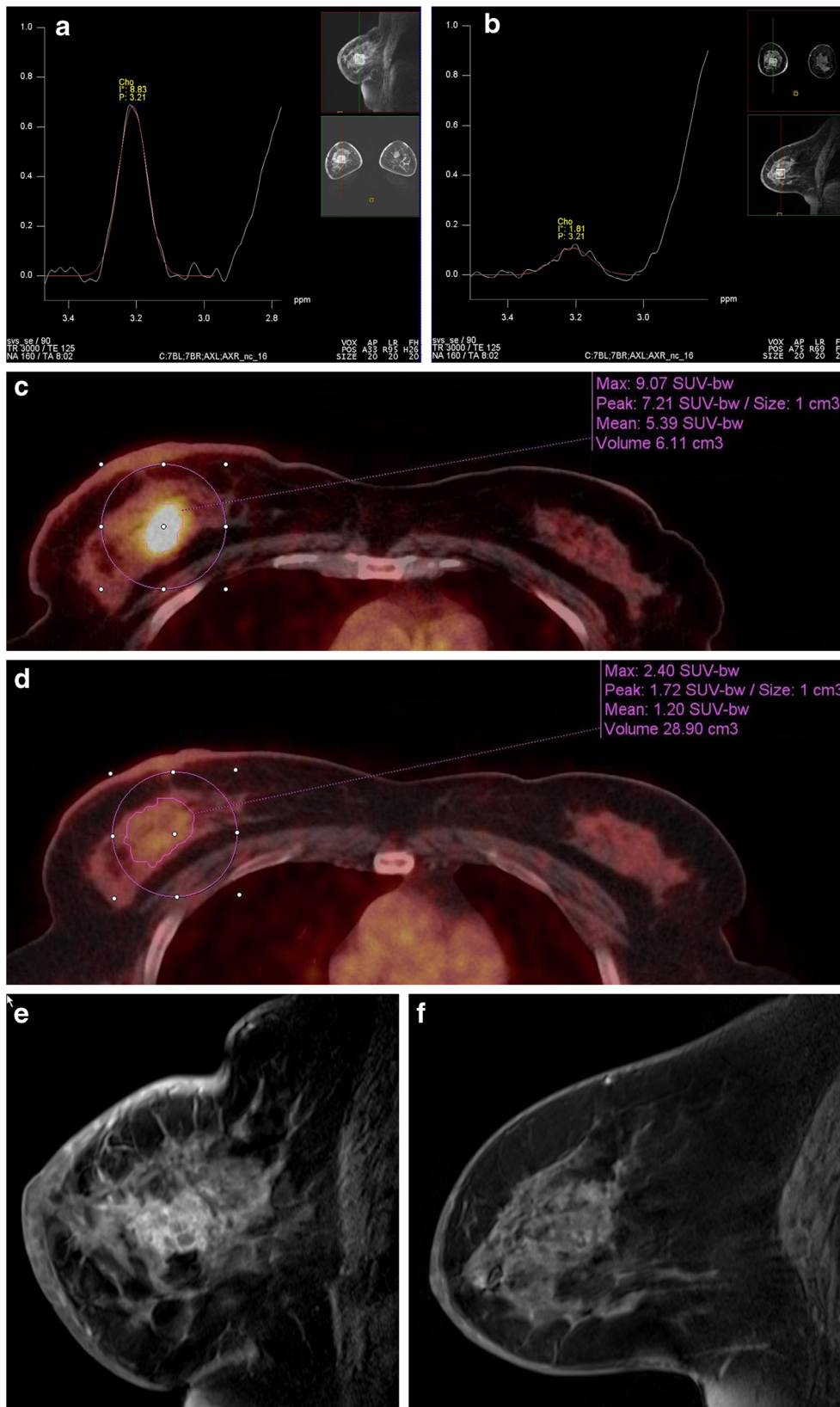
chemotherapy and tumour cellularity grade changes, MRS may be sufficiently sensitive to identify early changes of cellular proliferation from membrane choline phospholipid metabolism

changes in a similar degree to the early glucose metabolism changes observed with FDG-PET [29, 30]. Thus, our results demonstrate that MRS may be used as an alternative to FDG-

Fig. 2 Single-voxel ^{1}H-MR spectroscopy and ^{18}F-FDG-PET of a 53-year-old woman with invasive lobular carcinoma (ER+ and HER-2-negative) which were found to show a considerable amount of residual tumour after neoadjuvant chemotherapy and surgery. Pre-treatment (*A*) and post-1st cycle (*B*) single-voxel ^{1}H-MR spectrum shows that the normalized integral value of tCho resonance peak at 3.21 ppm decreased from 25.5 to 21.1, measured as a 17.3-% reduction. Pre-treatment (*C*) and post-1st cycle (*D*) SUV$_{max}$ of the tumour on FDG-PET decreased from 7.3 to 4.1, measured as a 43.8-% reduction. SUV$_{peak}$ of the tumour decreased from 5.1 to 2.9, measured as a 43.1-% reduction. Pre-treatment contrast-enhanced MRI (*E*) shows that the mass is 5.3 cm in diameter and preoperative contrast-enhanced MRI taken after completion of NAC shows the mass is 4.3 cm in diameter (*F*). Surgical histopathology revealed a 6.3-cm invasive lobular carcinoma. Miller-Payne classification was determined as a grade of 2, or a minor response
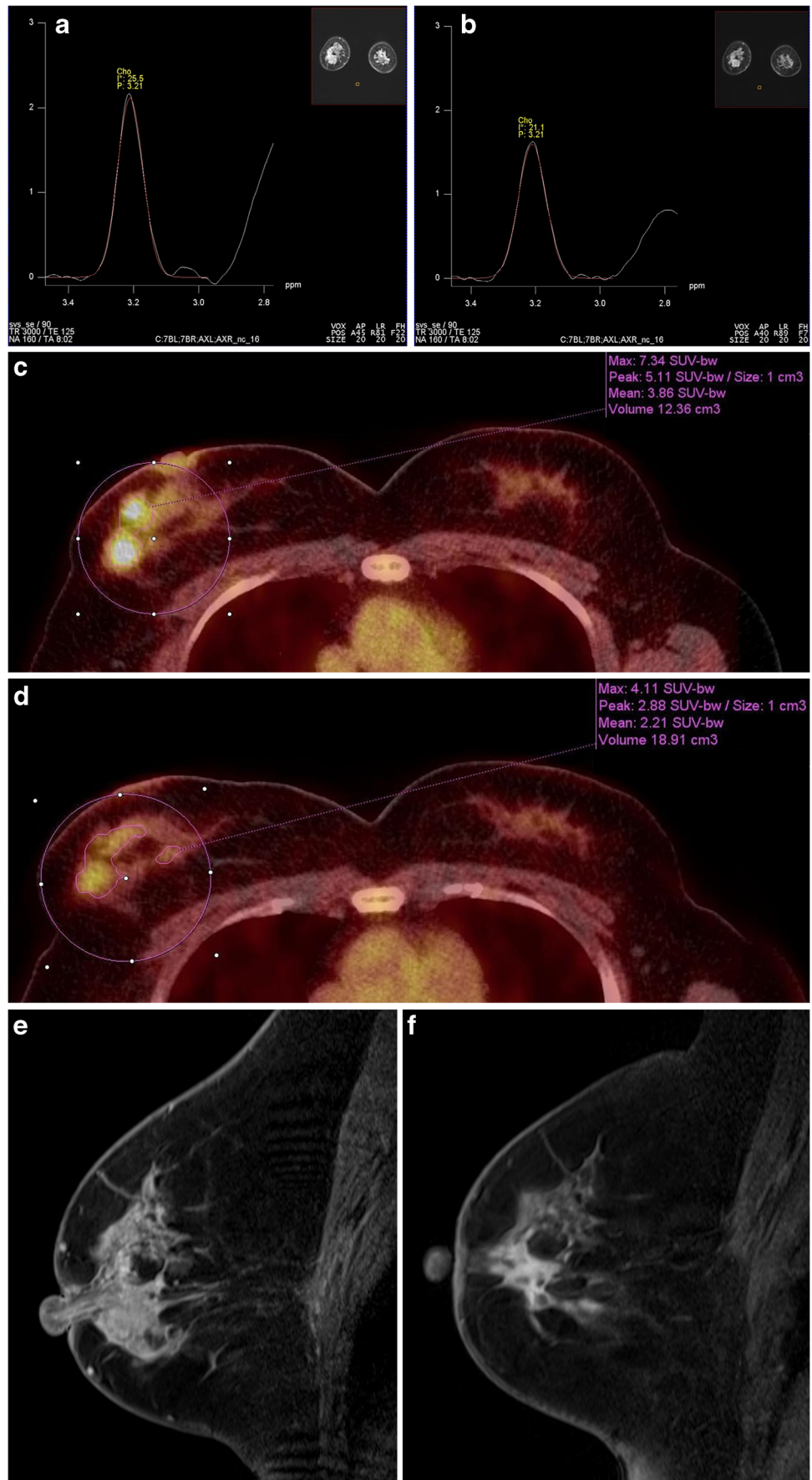
Fig. 3 Scatter plots demonstrate the results of linear regression between the % change of tumour size (*A*), % change of tCho at MRS (*B*), % change of SUV$_{max}$ (*C*), % change of SUV$_{peak}$ (*D*), % change of total lesion glycolysis (TLG) at FDG-PET (*E*), and Miller-Payne grades of cellular reduction, which resulted in significant correlations. For each scatter plot, the best-fit line is shown as a *solid line*
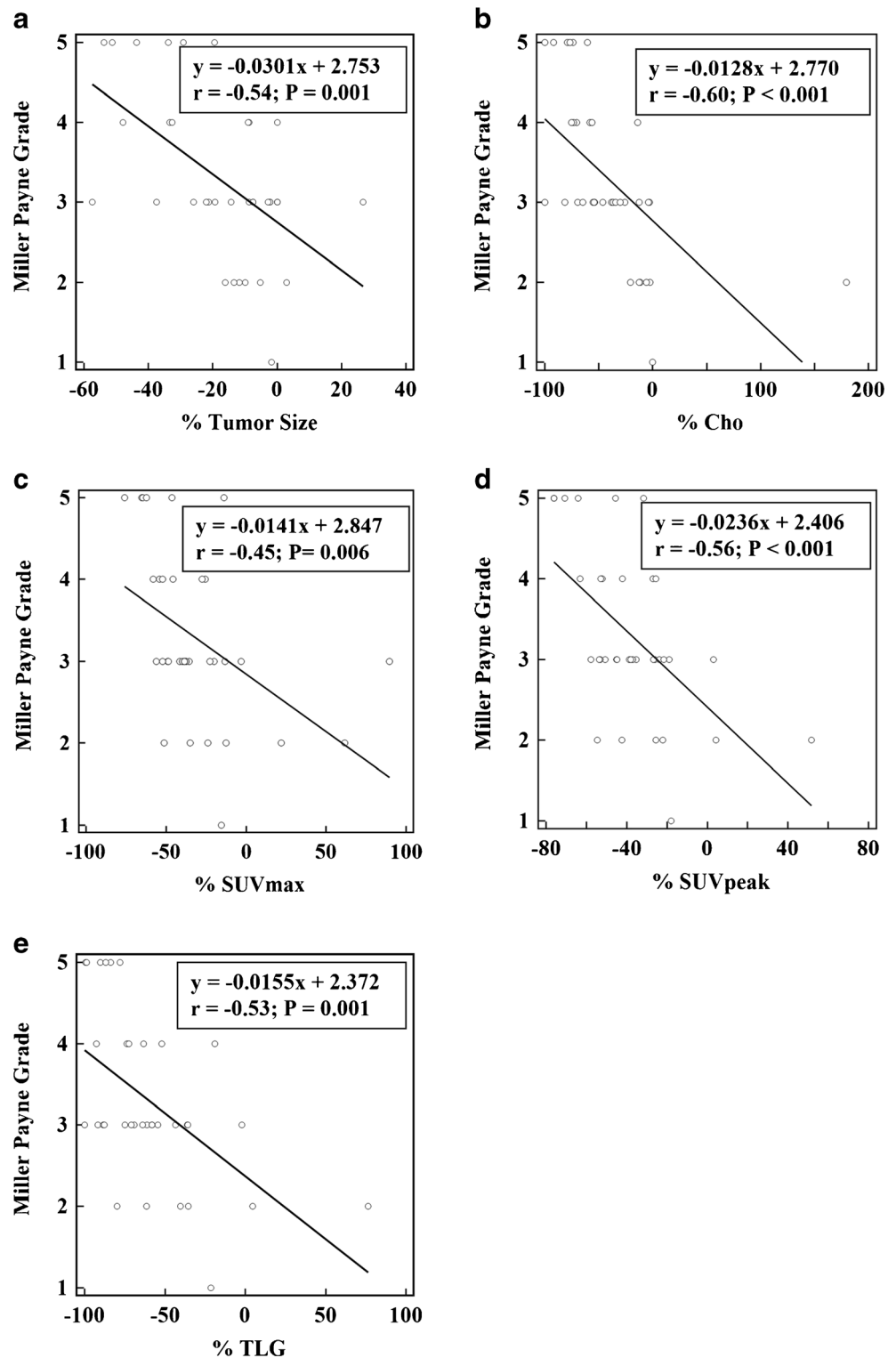
PET for the imaging prediction of the pathological response to NAC without additional ionizing radiation.

With regard to imaging parameter criteria, we analyzed the cut-off values in distinguishing not only pCR versus non-pCR but also good responders versus minor responders so as to avoid discontinuing an effective regimen in partial responders. When breast cancer patients receiving NAC present with a % tCho reduction lower than 25.7 %, modification of the regimen or alternative therapy may need to be considered as the patients would not respond to the regimen [100 % (7 of 7 minor responses) sensitivity]. To the contrary, when patients present a % tCho reduction of greater than 60.7 %, we can expect that
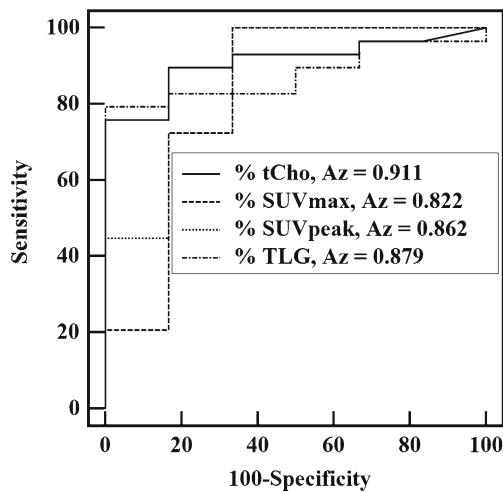
Fig. 4 Receiver operating characteristic curves evaluating the performances of MRS and FDG-PET in the prediction of non-pCR. The area under the ROC curve (Az) of % change of tCho was 0.911 (95 % CI, 0.765 to 0.980), which was similar to those of % change of SUV_{max} (0.822, 95 % CI, 0.656 to 0.930; P=0.552), SUV_{peak} (0.862, 95 % CI, 0.703 to 0.955, P=0.675), or TLG (0.879, 95 % CI, 0.725 to 0.965, P= 0.551). MRS = Single-voxel [1]H-MR spectroscopy, FDG-PET = ^{18}F-FDG-PET, pCR = pathologic complete response, tCho = otal choline-containing compounds, SUV = standardized uptake value, TLG = total lesion glycolysis

the patients would respond to NAC with 100 % (6 of 6 pCR) specificity. With regard to the cut-off values of FDG-PET in our study, a 35.6-% reduction of SUV_{max} yielded a sensitivity of 85.7 % (6/7 minor responses) and a specificity of 71.4 % (20/28 good responses). Although cut-off values can vary depending on the timing of the imaging (after 1st cycle versus 2nd cycle), the standard of reference (pCR versus histological grading versus survival outcome), and quantification methods (SUV versus metabolic rate), considering that cut-off values of 25-% to 45-% reduction in SUV_{max} at post-1st cycle of chemotherapy has been recommended by earlier studies [9, 31, 32], our study results are shown to be within the similar recommended
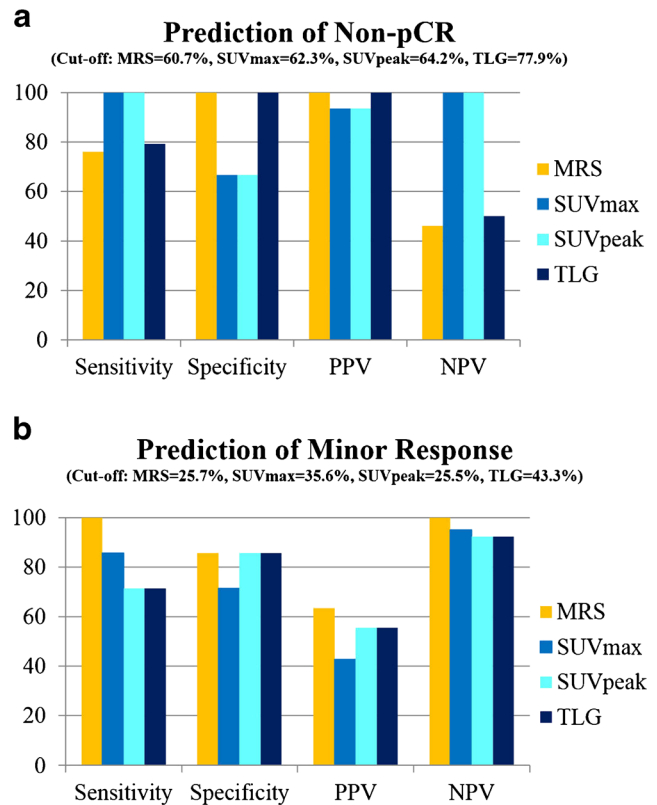
Fig. 5 Graphs demonstrating the sensitivity, specificity, positive predictive value (PPV), and negative predictive value (NPV) of single-voxel ^{1}H-MR spectroscopy (^{1}H-MRS), SUV_{max}, SUV_{peak}, and total lesion glycolysis (TLG) at ^{18}F-FDG-PET in the early prediction of non-pCR (*A*) and minor response (*B*)

range. With regard to the cut-off values of tCho, without standardization of acquisition and quantification methods of MRS for breast cancers, our cut-off tCho value may not be applicable to other institutions. Robust quantification methods for tCho using an external phantom reference or internal reference approach regardless of the voxel, magnetic field strength, breast coil design, or capability of shimming have been investigated in the

Table 3 Diagnostic performance of single-voxel [1]H-MR spectroscopy and ^{18}F-FDG-PET in the early prediction of non-pCR and minor responses

Performances	MRS	SUV_{max}	SUV_{peak}	TLG
Cut-off value in predicting non-pCR	60.7 %	62.3 %	64.2 %	77.9 %
Sensitivity	75.9 (22/29)	100 (29/29)	100 (29/29)	79.3 (23/29)
Specificity	100 (6/6)	66.7 (4/6)	66.7 (4/6)	100 (6/6)
Positive predictive value	100 (22/22)	93.5 (29/31)	93.5 (29/31)	100 (23/23)
Negative predictive value	46.2 (6/13)	100 (4/4)	100 (4/4)	50 (6/12)
Cut-off value in predicting minor response	25.7 %	35.6 %	25.5 %	43.3 %
Sensitivity	100 (7/7)	85.7 (6/7)	71.4 (5/7)	71.4 (5/7)
Specificity	85.7 (24/28)	71.4 (20/28)	85.7 (24/28)	85.7 (24/28)
Positive predictive value	63.6 (7/11)	42.9 (6/14)	55.6 (5/9)	55.6 (5/9)
Negative predictive value	100 (24/24)	95.2 (20/21)	92.3 (24/26)	92.3 (24/26)

Numbers represent percentages

MRS Single-voxel [1]H-MR spectroscopy, *FDG-PET* ^{18}F-FDG-PET, *pCR* Pathologic complete response, *TLG* Total lesion glycolysis

literature [33]. However, these absolute quantification methods are too complicated to be performed in routine clinical practice [34]. In our study, we used relative changes of the normalized integral value of the tCho peak before and after the 1st cycle of NAC, which has been shown to be accurate in discriminating malignant from benign lesions and which are more practical for clinical use [34]. Thus, we believe that relative quantification of normalized integral values of the tCho peak can be used as a parameter in longitudinal studies for the early prediction of the pathologic response to NAC.

Another interesting result of our study is that the Az value of TLG (0.879) was similar to those of SUV_{peak} (0.862) and SUV_{max} (0.822). Although SUV_{max} is simple and reproducible to obtain, however, as it only represents one pixel showing highest SUV, volume-based analysis such as TLG has been recommended in recent studies, which is consistent with our study results [17, 19].

The strengths of our study are the prospective application of imaging protocols, i.e., MRS and FDG-PET were acquired from the same patients with a mean interval of only 1 day, with consistent time points of imaging acquisition and chemotherapy regimens.

Nonetheless, our study has several limitations. First, this was a single institutional study with a relatively small sample size. Moreover, due to the higher number of dropouts than we expected, we only included 35 patients. Second, we did not assess the reproducibility of the quantification of integral values of the tCho peak on MRS. Third, the cut-off values for imaging parameters derived from our study population might have overestimated our results. Thus, further studies with a validation cohort may be warranted in future studies. Despite these limitations, we believe that our results showing that MRS provided similar predictive capabilities as FDG-PET can be of great clinical value.

In conclusion, our study demonstrated that MRS can be used as an alternative to FDG-PET in the early prediction of the pathological response to NAC in breast cancer patients, allowing response-guided treatment modification with comparable accuracy to FDG-PET without additional ionizing radiation.

References

1. Chia S, Swain SM, Byrd DR et al (2008) Locally advanced and inflammatory breast cancer. J Clin Oncol 26:786–790
2. Buchholz TA, Lehman CD, Harris JR et al (2008) Statement of the science concerning locoregional treatments after preoperative chemotherapy for breast cancer: a National Cancer Institute Conference. J Clin Oncol 26:791–797
3. Von Minckwitz G, Kaufmann M, Kuemmel S, for the GBG and AGO-B Study Groups et al (2011) Correlation of various pathologic complete response (pCR) definitions with long-term outcome and the prognostic value of pCR in various breast cancer subtypes: results from the German neoadjuvant meta-analysis. J Clin Oncol 29:1028
4. Kaufmann M, von Minckwitz G, Mamounas EP et al (2012) Recommendations from an international consensus conference on the current status and future of neoadjuvant systemic therapy in primary breast cancer. Ann Surg Oncol 19:1508–1516
5. von Minckwitz G, Blohmer JU, Costa SD et al (2013) Response-guided neoadjuvant chemotherapy for breast cancer. J Clin Oncol 31:3623–3630
6. Hylton NM, Blume JD, Bernreuter WK et al (2012) Locally advanced breast cancer: MR imaging for prediction of response to neoadjuvant chemotherapy–results from ACRIN 6657/I-SPY TRIAL. Radiology 263:663–672
7. Rieber A, Brambs HJ, Gabelmann A, Heilmann V, Kreienberg R, Kuhn T (2002) Breast MRI for monitoring response of primary breast cancer to neoadjuvant chemotherapy. Eur Radiol 12:1711–1719
8. Rousseau C, Devillers A, Sagan C et al (2006) Monitoring of early response to neoadjuvant chemotherapy in stage II and III breast cancer by [18F]fluorodeoxyglucose positron emission tomography. J Clin Oncol 24:5366–5372
9. Schwarz-Dose J, Untch M, Tiling R et al (2009) Monitoring primary systemic therapy of large and locally advanced breast cancer by using sequential positron emission tomography imaging with [18F]fluorodeoxyglucose. J Clin Oncol 27:535–541
10. Meisamy S, Bolan PJ, Baker EH et al (2004) Neoadjuvant chemotherapy of locally advanced breast cancer: predicting response with in vivo (1)H MR spectroscopy–a pilot study at 4 T. Radiology 233: 424–431
11. Baek HM, Chen JH, Nie K et al (2009) Predicting pathologic response to neoadjuvant chemotherapy in breast cancer by using MR imaging and quantitative 1H MR spectroscopy. Radiology 251:653–662
12. Danishad KKA, Sharma U, Sah RG, Seenu V, Parshad R, Jagannathan NR (2010) Assessment of therapeutic response of locally advanced breast cancer (LABC) patients undergoing neoadjuvant chemotherapy (NACT) monitored using sequential magnetic resonance spectroscopic imaging (MRSI). NMR Biomed 23: 233–241
13. Tozaki M, Sakamoto M, Oyama Y et al (2008) Monitoring of early response to neoadjuvant chemotherapy in breast cancer with (1)H MR spectroscopy: comparison to sequential 2-[18F]-fluorodeoxyglucose positron emission tomography. J Magn Reson Imaging 28:420–427
14. Cho N, Im SA, Park IA et al (2014) Breast cancer: early prediction of response to neoadjuvant chemotherapy using parametric response maps for MR imaging. Radiology 272:385–396
15. Tozaki M, Sakamoto M, Oyama Y, Maruyama K, Fukuma E (2010) Predicting pathological response to neoadjuvant chemotherapy in breast cancer with quantitative 1H MR spectroscopy using the external standard method. J Magn Reson Imaging 31:895–902
16. Wahl RL, Jacene H, Kasamon Y, Lodge MA (2009) From RECIST to PERCIST: evolving considerations for PET response criteria in solid tumors. J Nucl Med 50(Suppl 1):122S–150S
17. Lopci E, Zucali PA, Ceresoli GL et al (2015) Quantitative analyses at baseline and interim PET evaluation for response assessment and

outcome definition in patients with malignant pleural mesothelioma. Eur J Nucl Med Mol Imaging 42:667–675

18. Im HJ, Kim YK, Kim YI, Lee JJ, Lee WW, Kim SE (2013) Usefulness of combined metabolic-volumetric indices of (18)F-FDG PET/CT for the early prediction of neoadjuvant chemotherapy outcomes in breast cancer. Nucl Med Mol Imaging 47:36–43

19. Ogston KN, Miller ID, Payne S et al (2003) A new histological grading system to assess response of breast cancers to primary chemotherapy: prognostic significance and survival. Breast 12:320–327

20. Silver DP, Richardson AL, Eklund AC et al (2010) Efficacy of neoadjuvant Cisplatin in triple-negative breast cancer. J Clin Oncol 28:1145–1153

21. Jung SY, Kim SK, Nam BH et al (2010) Prognostic impact of [18F] FDG-PET in operable breast cancer treated with neoadjuvant chemotherapy. Ann Surg Oncol 17:247–253

22. Connolly RM, Leal JP, Goetz MP et al (2015) TBCRC 008: early change in 18F-FDG uptake on PET predicts response to preoperative systemic therapy in human epidermal growth factor receptor 2-negative primary operable breast cancer. J Nucl Med 56:31–37

23. Ah-See ML, Makris A, Taylor NJ et al (2008) Early changes in functional dynamic magnetic resonance imaging predict for pathologic response to neoadjuvant chemotherapy in primary breast cancer. Clin Cancer Res 14:6580–6589

24. Li SP, Makris A, Beresford MJ et al (2011) Use of dynamic contrast-enhanced MR Imaging to predict survival in patients with primary breast cancer undergoing neoadjuvant chemotherapy. Radiology 260:68–78

25. Tateishi U, Miyake M, Nagaoka T et al (2012) Neoadjuvant chemotherapy in breast cancer: prediction of pathologic response with PET/CT and dynamic contrast-enhanced MR imaging–prospective assessment. Radiology 263:53–63

26. Pengel KE, Koolen BB, Loo CE et al (2014) Combined use of ^{18}F-FDG PET/CT and MRI for response monitoring of breast cancer

during neoadjuvant chemotherapy. Eur J Nucl Med Mol Imaging 41:1515–1524

27. Lim I, Noh WC, Park J et al (2014) The combination of FDG PET and dynamic contrast-enhanced MRI improves the prediction of disease-free survival in patients with advanced breast cancer after the first cycle of neoadjuvant chemotherapy. Eur J Nucl Med Mol Imaging 41:1852–1860

28. An YY, Kim SH, Kang BJ, Lee AW (2015) Treatment response evaluation of breast cancer after neoadjuvant chemotherapy and usefulness of the imaging parameters of MRI and PET/CT. J Korean Med Sci 30:808–815

29. Aboagye EO, Bhujwalla ZM (1999) Malignant transformation alters membrane choline phospholipid metabolism of human mammary epithelial cells. Cancer Res 59:80–84

30. Glunde K, Bhujwalla ZM, Ronen SM (2011) Choline metabolism in malignant transformation. Nat Rev Cancer 11:835–848

31. Kolesnikov-Gauthier H, Vanlemmens L, Baranzelli MC et al (2012) Predictive value of neoadjuvant chemotherapy failure in breast cancer using FDG-PET after the first course. Breast Cancer Res Treat 131:517–525

32. Young H, Baum R, Cremerius U et al (1999) Measurement of clinical and subclinical tumour response using [18F]-fluorodeoxyglucose and positron emission tomography: review and 1999 EORTC recommendations. European Organization for Research and Treatment of Cancer (EORTC) PET Study Group. Eur J Cancer 35:1773–1782

33. Begley JK, Redpath TW, Bolan PJ, Gilbert FJ (2012) In vivo proton magnetic resonance spectroscopy of breast cancer: a review of the literature. Breast Cancer Res 14:207

34. Sardanelli F, Fausto A, Di Leo G, de Nijs R, Vorbuchner M, Podo F (2009) In vivo proton MR spectroscopy of the breast using the total choline peak integral as a marker of malignancy. AJR Am J Roentgenol 192:1608–1617